TITLE:

Substorm simulation: Quiet and N-S arcs preceding auroral breakup

AUTHOR(S):

Ebihara, Y.; Tanaka, T.

CITATION:

Ebihara, Y. ...[et al]. Substorm simulation: Quiet and N-S arcs preceding auroral breakup. Journal of Geophysical Research A: Space Physics 2016, 121(2): 1201-1218

ISSUE DATE:

2016-01-01

URL:

http://hdl.handle.net/2433/237231

RIGHT:

An edited version of this paper was published by AGU. Copyright 2016 American Geophysical Union.

京都大学学術情報リポジトリ
KURENAI 紅
Kyoto University Research Information Repository

京都大学 KYOTO UNIVERSITY
A Self-archived copy in
Kyoto University Research Information Repository
https://repository.kulib.kyoto-u.ac.jp
京都大学学術情報リポジトリ KURENAI 紅 Kyoto University Research Information Repository

AGU PUBLICATIONS
JGR
Journal of Geophysical Research: Space Physics

RESEARCH ARTICLE
10.1002/2015JA021831

Key Points:
- Auroral arcs (N-S and quiet arcs) preceding breakup are reproduced by global MHD simulations
- The auroral arcs are manifestations of the structured high-pressure region in the high latitude
- The high-pressure region is structured by instability involved in magnetosphere-ionosphere coupling

Correspondence to:
Y. Ebihara,
ebihara@rish.kyoto-u.ac.jp

Citation:
Ebihara, Y., and T. Tanaka (2016), Substorm simulation: Quiet and N-S arcs preceding auroral breakup, *J. Geophys. Res. Space Physics*, *121*, 1201–1218, doi:10.1002/2015JA021831.

Received 21 AUG 2015
Accepted 8 JAN 2016
Accepted article online 11 JAN 2016
Published online 8 FEB 2016

©2016. American Geophysical Union. All Rights Reserved.

Substorm simulation: Quiet and N-S arcs preceding auroral breakup

Y. Ebihara[1] and T. Tanaka[2]

[1]Research Institute for Sustainable Humanosphere, Kyoto University, Kyoto, Japan, [2]International Center for Space Weather Science and Education, Kyushu University, Fukuoka, Japan

Abstract Auroral breakup at the onset of substorm expansion is sometimes preceded by auroral forms known as quiet arcs and N-S arcs. Observations have shown that both the auroral forms tend to move equatorward, and the initial brightening takes place in or near one of the quiet arcs. The auroral forms attract great attention, but generation of auroral forms and their association with the initial brightening are poorly understood. Recent global magnetohydrodynamic simulations are capable of producing upward field-aligned currents (FACs) that resemble the auroral forms in both shape and temporal evolution. Based on the simulation results, we propose the following scenarios: (1) When the convection electric field is weak (northward interplanetary magnetic field (IMF)), the high-pressure region is elongated from the plasma sheet toward higher latitudes and is structured by a coupling between the magnetosphere and the ionosphere (interchange-like instabilities). (2) When the convection electric field is strong (southward IMF), the structured high-pressure region moves equatorward (toward the plasma sheet). Upward currents are generated around it, which can be observed as arcs in the ionosphere. The upward current can be tentatively intensified in the course of the equatorward movement before the formation of a near-Earth neutral line (NENL). (3) The NENL releases magnetic tension and results in the enhancement of plasma pressure at off-equator in the near-Earth region. Sudden formation of the off-equatorial high-pressure region generates the onset current system that manifests initial brightening. Our scenario can explain the observational fact that poleward arcs remained undisturbed at the onset.

1. Introduction

It is widely believed that a precursor or preconditioning stage occurs before the onset of substorm expansion, which is called the growth phase [*McPherron*, 1970; *Akasofu and Snyder*, 1972, and references therein]. Magnetospheric manifestations of the growth phase include the thinning of the plasma sheet, and a change in the configuration of the geomagnetic field, from dipolar to tail-like near the geosynchronous orbit. Ionospheric manifestations of the growth phase include a slow growth of magnetic disturbance at auroral latitudes, a growth of current system in the polar cap, a growth in the westward electric field, and an equatorward motion of auroras. It is commonly thought that the growth phase begins when the interplanetary magnetic field (IMF) turns southward [e.g., *Kokubun*, 1971] and starts to store energy, although there are some minor exceptions, in which the onset of the substorm expansion occurs in the absence of a southward turning of the IMF [e.g., *Kamide*, 1974]. *Kamide and Matsushita* [1978] suggested that the probability of an onset increases with available energy stored in the tail region.

1.1. Quiet Arcs

The substorm expansion phase starts with a sudden brightening of one of the longitudinally elongated quiet arcs and subsequent poleward motion [*Akasofu*, 1964]. Some auroral activities preceding the onset of substorm expansion have been recognized as precursor phenomena and reflection of the fundamental processes leading to the onset. One of such auroral activity is the quiet and homogeneous arc [*Akasofu*, 1964] (hereinafter, referred to as a quiet arc). The quiet arc tends to lie longitudinally, and multiple quiet arcs are also observed to form within the auroral oval before the onset of substorm expansion [e.g., *Akasofu*, 1964; *Haerendel et al.*, 2012]. These quiet arcs have a thickness of around 100 km [*Johnson et al.*, 1998] and move equatorward at a speed of 2–6 km min^{-1}, which is consistent in part with convective motion [*Lassen et al.*, 1977; *Haerendel et al.*, 2012]. The electron precipitation has a sharp poleward boundary, and the boundary moves equatorward when the IMF is turned southward [*Hoffman and Burch*, 1973]. The quiet arcs are caused by precipitating electrons with a peak energy of approximately 1–5 keV, so that they are most likely accelerated by electric fields parallel

京都大学 KYOTO UNIVERSITY
A Self-archived copy in
Kyoto University Research Information Repository
https://repository.kulib.kyoto-u.ac.jp
京都大学学術情報リポジトリ KURENAI 紅 Kyoto University Research Information Repository

to magnetic field lines [*Meng*, 1976; *Lassen et al*., 1977; *Haerendel et al*., 2012]. *Lessard et al*. [2007] investigated data from ground-based auroral imagers and the Fast Auroral Snapshot Explorer (FAST) satellite. They found that quiet arcs develop within the region of proton precipitation, and that these arcs are excited by electrons accelerated by parallel electric fields. Quiet arcs are also accompanied by upward field-aligned currents (FACs) [*Jiang et al*., 2012]. In the premidnight region, most quiet arcs are observed less than 1° poleward of the boundary between Regions 1 and 2 currents [*Jiang et al*., 2015]. Flow shear is present in the ionosphere, both near the quiet arcs [*Marklund*, 1984; *Timofeev and Galperin*, 1991], and in the topside ionosphere [*Jiang et al*., 2015]. This flow shear is consistent with the convergence of the Pedersen currents (the converging electric field [*Johnson et al*., 1998]) that are connected with the upward FAC in the ionosphere. The quiet arcs are known by a number of different names, including evening anticorrelation arcs [*Marklund*, 1984], growth phase arcs [*Lyons et al*., 2000, 2011; *Haerendel*, 2010; *Nishimura et al*., 2012], preexisting arcs [*Jiang et al*., 2012], and a quiet evening arcs [*Coroniti and Pritchett*, 2014].

Two different types of electron precipitation have been proposed to explain the formation of quiet arcs. The first type of precipitation is associated with earthward acceleration of electrons by parallel electric fields. The other type is associated with scattering in the plasma sheet. The former type of precipitation is supported by observational evidence [*Meng*, 1976; *Lessard et al*., 2007; *Jiang et al*., 2012, 2015]. The existence of parallel electric fields may lead to the speculation of an associated upward FAC, because a necessary condition for the appearance of parallel electric fields is an upward FAC [*Mozer and Hull*, 2001]. A statistical study of the relationship between FACs and electron precipitation revealed that at dusk, upward FACs are well correlated with the precipitation of electrons accelerated downward by parallel electric fields [*Korth et al*., 2014]. *Jiang et al*. [2012] provided direct observational verification of this mechanism. The upper end of the auroral acceleration region is suggested to be located at an altitude of 3.0–3.5 *Re* at 20–24 magnetic local time (MLT) [*Mozer and Hull*, 2001]. After being accelerated in a parallel direction, the electrons will move along a field line and collide with atoms and molecules in the thermosphere, resulting in an auroral arc. If this is the case for the quiet arc, the quiet arc will represent a projection of magnetospheric processes at the acceleration region probably located at an altitude of 3.0–3.5 *Re*. In this way, the FAC is the primary cause of the particle precipitation that forms the arc, and understanding the generation of the FAC is important in understanding the arc itself. Previously, it has been thought that the FAC is connected to the equatorial plane in the near-Earth plasma sheet along a field line. As such, the near-Earth plasma sheet has been believed to be the generation region for the FACs. By considering the necessary current continuity, azimuthal pressure gradients in the near-Earth plasma sheet may act to generate and close the upward FACs that are associated with the quiet arcs [*Lyons and Samson*, 1992; *Antonova*, 1993; *Stepanova et al*., 2002; *Haerendel*, 2007; *Coroniti and Pritchett*, 2014]. To explain the narrowness of the quiet arcs, *Galperin et al*. [1992] and *Galperin and Bosqued* [1999] suggested that the plasma pressure can be localized in the radial direction by a loss of ions due to pitch angle scattering in the region where the radius of curvature of the magnetic field line is small compared with the gyroradius of the ion. This is known as field line curvature (FLC) scattering.

The second type of electron precipitation is derived from the idea that electrons can be precipitated by the FLC scattering [*Yahnin et al*., 1997]. In this way, the electron precipitation itself is the cause of the FAC. Although electrons precipitating in this way may be sufficient to sustain the upward FAC [*Sergeev et al*., 2011], it is as yet unclear how the current is closed within the magnetosphere, and how the velocity space distribution of precipitating electrons can be explained by FLC scattering.

The magnetosphere-ionosphere coupling is also thought to be important in creating multiple quiet arcs, in terms of ionospheric closure by polarization currents [*Atkinson*, 1970], cross-field instability [*Ogawa and Sato*, 1971], feedback instability [*Sato*, 1978; *Watanabe et al*., 1986; *Lysak and Song*, 2002; *Hasegawa et al*., 2010], field line resonance [*Rankin et al*., 1999; *Streltsov and Lotko*, 1995; *Lotko et al*., 1998], and the nonlinear evolution of Alfvén waves [*Lysak and Dum*, 1983]. Shear flows in the transition layer, spanning the low-latitude boundary layer and the magnetosphere, have been suggested to generate an electrostatic parallel electric field that accelerates electrons downward [*Lyons*, 1980; *Roth et al*., 1993; *Echim et al*., 2009].

1.2. N-S Arcs

In addition to quiet arcs, other kinds of auroral forms have also been recognized as the auroral activities that precede the auroral breakup. *Oguti* [1973] identified a contact breakup, in which a longitudinally elongated arc splitting from the high-latitude arc contacts with the proton aurora, triggering the beginning of the

京都大学 KYOTO UNIVERSITY
A Self-archived copy in
Kyoto University Research Information Repository
https://repository.kulib.kyoto-u.ac.jp
京都大学学術情報リポジトリ KURENAI 紅 Kyoto University Research Information Repository

breakup. *Kadokura et al*. [2002] identified the fast equatorward moving (FEM) arcs that appear around 20 min before the onset of substorm expansion on the high-latitude side of the auroral region. These FEM arcs are identified as discrete auroral forms and are longitudinally elongated. *Kadokura et al*. [2002] also found an auroral form that appears a few minutes before onset in the poleward most region at wavelength of 630.0 nm. They termed it the near plasma sheet boundary layer aurora. *Kepko et al*. [2009] utilized data from multispectral all-sky imagers at 427.0, 557.7, and 630.0 nm and found a diffuse equatorward moving patch at 630.0 nm and a narrow discrete form at 557.7 nm just before the onset. The discrete form at 557.7 nm lies near the westward edge of the diffuse patch at 630.0 nm, and the auroral form and diffuse patch both appear poleward of the onset arc location. *Nishimura et al*. [2010] performed a statistical study on the equatorward moving discrete form that appears prior to the onset. They found that onset tends to occur when a discrete arc reaches the equatorward portion of the auroral oval. According to their study, 34% of the preonset N-S arcs are east-west aligned, 48% of them are north-south aligned, and 19% is switched from north-south to east-west alignments over the course of their propagation from high latitudes to the auroral oval. Hereinafter, we call them the N-S arc for simplicity.

Kepko et al. [2009] identified a diffuse patch at 630.0 nm and a discrete auroral form at 557.7 nm. They suggested that the diffuse patch represents the ionospheric footprint of an earthward moving flow burst in the midtail plasma sheet and that the discrete form corresponds an upward FAC connecting with the west side of the earthward flow burst [*Kepko et al*., 2004]. In this respect, they suggested that the N-S arcs are similar to streamers that are found after the onset and are associated with earthward fast flows in the plasma sheet [*de la Beaujardière et al*., 1994; *Henderson et al*., 1998; *Lyons et al*., 1999; *Sergeev et al*., 1999, 2000; *Zesta et al*., 2000; *Nakamura et al*., 2001]. On the analogy of the streamers that appear after the onset, the N-S arcs are believed to reflect the processes in the plasma sheet [*Nishimura et al*., 2010, 2011] that lead to the formation of the substorm current wedge (SCW) [*McPherron et al*., 1973]. *Nishimura et al*. [2010] and *Lyons et al*. [2010] suggested that the formation of the SCW is not spontaneous, and that it is caused by disturbances propagating from the downtail region. It is evident that two-dimensional auroral imaging can provide a unique opportunity to clarify substorm sequences in the magnetosphere and to compensate for the limitations of satellite observations in that an entire sequence cannot be observed at once [e.g., *Kepko et al*., 2009; *Nishimura et al*., 2010]. However, some questions still remain unanswered. First, streamers are seen not only around the onset but also during the expansion phase and even during the quiet period. Therefore, it is not clear why a particular streamer leads to onset. Second, an intrusion of new, low-entropy plasma into the inner edge of the electron plasma sheet is suggested to trigger certain instabilities [*Nishimura et al*., 2010; *Lyons et al*., 2010]. It remains to be determined which types of instability must be selectively present for the onset of substorm expansion.

1.3. Onset

A sudden brightening of one of the quiet arcs is considered to be an ionospheric manifestation of the onset of the polar substorm. Thus, the quiet arc that begins to intensify at the onset has been given particular research attention. The sudden brightening of the aurora is associated with a sudden intensification of the upward FAC. Since the early 1970s, these upward FACs have been thought to be a part of the SCW. The SCW has commonly been regarded as the prime current system that leads to the onset of substorm expansion [*Kepko et al*., 2014, and references therein]. Based on the mapping of quiet arcs to the equatorial plane along model magnetic field lines, the arcs are most plausibly mapped to a radial distance of 6–10 *Re* [*Samson et al*., 1992], or 7–8 *Re* on a closed magnetic field, and no further than 12 *Re* [*Donovan et al*., 2008]. Most of the recent substorm researches over the last two decades have assumed, as a prerequisite, that the study of auroral substorm onset is equivalent to the study of the formation of the SCW. A number of mechanisms have been proposed to explain the generation of the SCW, such as a disruption of the cross-tail current by instabilities [*Lui*, 1996], inertial currents [*Shiokawa et al*., 1997], azimuthal pressure gradients [*Shiokawa et al*., 1998; *Birn et al*., 1999; *Yao et al*., 2012], flow vortices near the equatorial plane [*Birn et al*., 2004; *Keiling et al*., 2009], and low-entropy magnetic flux tubes or plasma bubbles [*Sergeev et al*., 1996; *Chen and Wolf*, 1999; *Nakamura et al*., 2001; *Birn et al*., 2004; *Xing et al*., 2011].

1.4. Simulation Studies

Global magnetohydrodynamics (MHD) simulations are capable of reproducing some structure and dynamics of the magnetospheric processes that are key for understanding observed aspects of substorms and storms. For instance, *Hesse and Birn* [1994] simulated earthward propagating fast flows and enhancements of

京都大学 KYOTO UNIVERSITY
A Self-archived copy in
Kyoto University Research Information Repository
https://repository.kulib.kyoto-u.ac.jp
京都大学学術情報リポジトリ KURENAI 紅 Kyoto University Research Information Repository

magnetic field that is denoted as dipolarization fronts [e.g., *Nakamura et al.*, 2002]. *Wiltberger et al.* [2000] showed that the simulation result agrees with single-point substorm-time observations acquired by satellites. *Raeder et al.* [2001] compared their simulation results with ground disturbances of the magnetic field, ionospheric electric potential patterns, and magnetic and plasma data obtained by the GOES and Geotail satellites for the substorm event of 24 November 1996. An isolated substorm of 9 March 1995 was simulated by *Lyon et al.* [1998] who calculated magnetic disturbances caused by auroral electrojet. They emphasized the importance of an electric field spike penetrating into the near-Earth region. *Ohtani and Raeder* [2004] found a tailward moving surge of the tail current in the simulation result and compared with data from the Interball and IMP 8 satellites. Global precipitation pattern of magnetospheric electrons was compared with global auroral images by *Palmroth et al.* [2006]. *Tóth et al.* [2007] succeeded to simulate a response of the magnetosphere even to the huge coronal mass ejection that took place in October 2003. Ground observations can also be reproduced from the simulation. *Yu et al.* [2010] evaluated contributions from the magnetospheric currents, the FAC, and the ionospheric Hall and Pedersen currents to the ground disturbance of the magnetic field. The contribution from the ionospheric Hall current dominates at high altitudes, whereas the magnetospheric currents and FACs contribute mostly to the total disturbance at low and middle latitudes. *Ge et al.* [2011] showed fine structures of earthward bursty bulk flows (BBFs) in the plasma sheet. The BBFs are diverted eastward and westward, generating the FACs that are responsible for auroral brightening.

Recently, it has been presented that the finer the spatial resolution of the global magnetohydrodynamic (MHD) simulations, which consider the effects of the magnetosphere-ionosphere (M-I) coupling, the more realistic the features of the auroral or polar substorms that can be reproduced [*Tanaka et al.*, 2010; *Ebihara et al.*, 2014; *Tanaka*, 2015, hereinafter referred to as Paper 1; *Ebihara and Tanaka*, 2015a, Paper 2; *Ebihara and Tanaka*, 2015b, Paper 3]. In these precise simulations, ionospheric elements of substorms, such as the sudden decrease in the Auroral Lower (*AL*) index, the quiet arc, the dipolarization front, the initial brightening, the westward traveling surge (WTS), the double oval, and the overshielding, are reproduced. One of the most important findings of recent global M-I coupling simulations is the presence of a near-Earth high-pressure region that generates a Region 1-sense FAC. The role of the SCW in intensifying the upward FAC that manifests during the initial brightening is questionable in the simulation because the dawn-dusk cross-tail current cannot be connected with the ionosphere as a Region 1-sense FAC. This is due to the fact that the current lines are diverted from the magnetic field line by the strong perpendicular current flowing near the plasma sheet. The underlying mechanisms for onset of auroral substorms are linked to the near-Earth high-pressure region that is formed by transition between force balance states in the plasma sheet in association with changes in large-scale convection [*Tanaka et al.*, 2010]. This may represent a paradigm shift for the substorm onset model, from the SCW to the near-Earth high-pressure region. If the near-Earth high-pressure region plays an essential role in the onset, then the context of the onset may be able to be understood in the framework of the MHD (Paper 2).

After confirming the successful reproduction of many aspects of a polar substorm, the global M-I coupling simulation has recently been applied to the study of quiet arcs (Paper 1). If the proton aurora is regarded as the high-pressure region with the Region 2 current, then the proton aurora will be mapped, along a field line, to the plasma sheet region around its inner boundary (7–12 *Re*), and the quiet arc is mapped to the region beyond there, ranging from 12 *Re* to the lobe-plasma sheet boundary. On the other hand, the current lines extending from the quiet arc are connected to the lobe-plasma sheet boundary, which is, in part, consistent with the observation that the lobe-plasma sheet boundary region acts as a dynamo [*Marghitu et al.*, 2006; *Hamrin et al.*, 2006]. When one maps the plasma sheet to the ionosphere along a field line, the mapped area is narrower than expected. For example, a vast area from the near-Earth neutral line (NENL; near 20 Re) to the inner boundary of the plasma sheet (for instance, 7 *Re*) is projected only to a few degrees of latitude in the ionosphere, due to the stretched magnetic field lines. Such stretched magnetic field lines in the growth phase were also presented by adapted empirical magnetic field models [e.g., *Pulkkinen*, 1991; *Pulkkinen et al.*, 1991, 1994; *Kubyshkina et al.*, 2011] and simulations [e.g., *Pritchett and Coroniti*, 1995, 1997; *Hesse et al.*, 1996].

Traditionally, the N-S arcs have also been regarded as ionospheric projections of plasma sheet processes [*Kepko et al.*, 2009; *Nishimura et al.*, 2010, 2011; *Mende et al.*, 2011]. The latitudinal width between the poleward edge of the N-S arc and the equatorward edge of the auroral oval can exceed 10° of magnetic latitude [*Mende et al.*, 2011; *Nishimura et al.*, 2013]. However, such thickness of the auroral oval would be too wide to be explained in terms of the ionospheric projection of the plasma sheet along a field line if the magnetic field

京都大学 KYOTO UNIVERSITY
A Self-archived copy in
Kyoto University Research Information Repository
https://repository.kulib.kyoto-u.ac.jp
京都大学学術情報リポジトリ KURENAI 紅 Kyoto University Research Information Repository

lines were highly stretched, as previously suggested. It should be emphasized that the current lines must be considered primarily, and that the current line can be easily diverted from the magnetic field line [*Birn and Hesse*, 1996; *Tanaka et al*., 2010]. In this way, the auroral structure is not always a simple projection of the plasma sheet, due to the presence of the strong perpendicular current. During the initial brightening (Paper 2) and the westward traveling surge (WTS) (Paper 3), the current lines extending from these auroral forms are connected with the cusp-mantle dynamo via the near-Earth high-pressure region that is newly developed near the onset. Thus, there is no guarantee that the quiet arcs and the N-S arcs represent simple projections of plasma sheet processes as previously expected. These possibilities are also shown by Paper 1. If the auroral activities that take place before the onset (such as quiet arcs and N-S arcs) are not a simple projection of the plasma sheet, then it will be inevitable to reconsider their mechanisms other than plasma sheet processes. The purpose of this study is to provide new interpretations for the development of quiet arcs and N-S arcs, and their unified view based on the results of a global MHD simulation. In this study, we argue about the compound sequence of auroral generation processes, such as the generation of convection shear, the generation of the FAC, the formation of parallel electric field, and the excitation of quiet arcs and N-S arcs. Although the global MHD simulation cannot directly deal with the formation of a parallel electric field and the excitation of auroral luminosity, we can represent the auroral activities in the ionosphere, including quiet arcs and N-S arcs, from the upward FAC and the plasma pressure.

2. Simulation Setup

It is the grid structure that has the most effective influence on the performance of the global simulation. The most significant advantage of the present MHD simulation is to use a large-scale unstructured grid system having no apparent singularity. The generation of this grid system is based on a sphere with an inscribed dodecahedron [*Moriguchi et al*., 2008; *Nakamizo et al*., 2009; *Terada et al*., 2009]. First, one pentagonal surface of dodecahedron is divided into five triangles, and then each triangle is divided into four smaller triangles. Similar process continues. Finally, 122,886 grid points (245,760 triangles) are obtained on a sphere after 7 times of division. The three-dimensional grid system is generated by radially stacking 360 triangular prisms. The number of grid points is 46,572,278. We also assign 122,886 grid points to the ionosphere. Spatial resolution is about 0.5° in latitude in the ionosphere. Inner and outer boundaries for the magnetospheric calculation are at 3.0 *Re* and 300 *Re*, respectively. The grid structure is unchanged throughout the calculation.

In the magnetosphere, we solved the modified MHD equations such that the magnetic field **B** was divided into the dipole magnetic field $\mathbf{B}_0$ and deviation $\mathbf{B}_1$ [*Tanaka*, 1994]. This equation was integrated by adopting the finite volume total variation diminishing scheme. In this calculation, control volume is hexagonal or pentagonal columns. In the ionosphere located at the geocentric distance of 1 *Re*, the electric potential was calculated from the current continuity condition by adopting the MHD variables projected from the inner boundary to the ionosphere along the dipole magnetic field. The ionospheric conductivity was assumed to consist of three components. The first component depends on the solar zenith angle. The second component depends on the projected FAC. The third component depends on the projected pressure and projected temperature [*Tanaka et al*., 2010; *Ebihara et al*., 2014]. We assumed that the Hall conductivity is 3 times higher than the Pedersen conductivity throughout the calculation. The inner boundary of the magnetospheric domain is located at 3 *Re*, so that the MHD variables together with the grid structure were mapped to the ionosphere at latitudes higher than 54.3°. To obtain the electric potential from pole to pole, another grid system was connected to the projected grid system at 54.3° to extend the solution to the lower latitude region. An elliptic partial differential equation was solved by adopting the conjugate residual method. The obtained potential was mapped back to the inner boundary of the magnetospheric domain along the dipole magnetic field. The plasma velocity equivalent to the mapped electric field was imposed to the inner boundary of the magnetospheric domain for the purpose of establishing the M-I coupling process.

All of the simulation settings and parameters hitherto presented are identical to those in Paper 3. The simulation domain is uniform at the beginning of the simulation. We first set the solar wind density of 5.0 cm^{-3}, the solar wind speed of 372 km s^{-1}, the *Y* component of the interplanetary magnetic field (IMF B_y) of 2.5 nT, and the IMF B_z of 4.3 nT and calculated for 2 h. IMF B_x was held to be 0 throughout the calculation. At the elapsed time of 2 h, the magnetosphere exhibits the null separator topology suggested by *Tanaka et al*. [2010]. We then changed IMF B_z to −3.0 nT. We defined $t = 0$ as the moment at which the southward IMF reached

京都大学 KYOTO UNIVERSITY
A Self-archived copy in
Kyoto University Research Information Repository
https://repository.kulib.kyoto-u.ac.jp
京都大学学術情報リポジトリ KURENAI 紅 Kyoto University Research Information Repository

$X = 40\ Re$. At $t = 0$, the variation of the magnetosphere is slow enough to be regarded as a quasi-steady condition. As mentioned below, the magnetosphere does not reach the steady condition exactly because of the interaction between the magnetosphere and the ionosphere. The southward IMF reached the bow shock at the subsolar point at approximately $t = 6$ min. We have confirmed that simulation results are qualitatively the same for those with similar parameters, for instance, for the polarity of IMF B_y, the magnitude of IMF, solar wind speed, and density.

3. Results

3.1. Ionospheric Signatures of Quiet and N-S Arcs

Figure 1 shows the calculated Auroral Upper (*AU*) and Lower (*AL*) indices, and the FAC as a function of the magnetic latitude (MLAT) and time at 22 MLT in the Northern Hemisphere. The *AU* and *AL* indices were calculated based on the north-south component of the magnetic disturbance caused by the Hall current flowing in the ionosphere. The points used to calculate the *AU* and *AL* indices are located at 70 MLAT and at 24 different MLTs. They are equally spaced in MLT. At high latitudes, the contribution from the Hall current is most significant [*Yu et al*., 2010], so that the contribution from the Pedersen current and the FAC may be negligible. Of course, the *AU* and *AL* indices depend on the points used to calculate the magnetic disturbance. For the purpose of demonstrating the development of the auroral electrojet clearly, we selected 70 MLAT for this particular study. Four vertical lines are drawn in Figure 1. From left to right, they indicate the arrival of the southward IMF at the dayside magnetosheath (around $t = 6$ min), the enhancement of the DP2 ionospheric convection [*Nishida*, 1968] (around $t = 24$ min), the formation of the near-Earth neutral line (NENL) (around $t = 56$ min), and the initial brightening (sudden increase in the upward FAC near midnight(around $t = 70$ min). In the present study, we focus on the sequence taking place before the initial brightening. Paper 3 describes the sequence from the initial brightening onward, including initial brightening and WTS.

Around $t = 0$, the overall variation of the magnetosphere is slow enough to be regarded as a quasi-steady condition. Upward FAC regions reside around 70 MLAT and at >78 MLAT, but they move poleward slowly. When the ionosphere is affected by a southward IMF and the DP2 ionospheric convection is established, a part of the upward FAC region moves equatorward. After about 10 min later, the other part of the upward FAC region appears at around 80 MLAT and moves equatorward. The intensity of the upward FAC is temporarily enhanced while it resides in the high latitudes. The upward FAC is also enhanced at around 70 MLAT. The high-latitude parts of the upward FAC seem to merge with the low-latitude part between around $t = 50$ and 65 min. Shortly thereafter, the initial brightening occurs at late MLTs at around $t = 69.5$ min. A WTS is developed, which traverses the meridian at 22 MLT at around $t = 77$ min. The temporal and spatial variations in the upward FAC seem to be consistent with observations (e.g., Plate 2 of *Brittnacher et al*. [1999] and Figure 3 of *Nishimura et al*. [2011]).

Figure 2 shows FACs in the ionosphere in the Northern Hemisphere. When the IMF is northward, some structured regions of upward FACs are found at high latitudes. These upward FAC regions are elongated from the nightside to the dayside. Hereinafter, for simplicity, we describe an elongated-upward FAC region as an arc. Some of the arcs are approximately aligned toward the Sun and may be regarded as Sun-aligned arcs that appear when the IMF B_z is positive or is close to zero [*Davis*, 1962; *Ismail et al*., 1977; *Lassen and Danielsen*, 1978; *Ismail and Meng*, 1982; *Eliasson et al*., 1987; *Valladares et al*., 1994; *Shiokawa et al*., 1995, 1997; *Newell et al*., 1997]. For simplicity, we call them N-S arcs, although the N-S arcs are not always aligned toward the Sun. The arcs tend to move in accordance with the convection (along the contour of the electric potential). The pattern of electric potential is essentially consistent with a round convection cell [*Tanaka*, 2007]. However, the pattern is somewhat skewed and is distorted in the vicinity of the region where the amplitude of FAC is relatively large. The primary reason for this distorted electric potential pattern is that the electric potential tends to decrease where the upward FACs flow, and vice versa. A longitudinally elongated arc is found at ~70 MLAT on the nightside (Figure 2b). For simplicity, we call it a quiet arc [e.g., *Akasofu*, 1964; *Johnson et al*., 1998]. When the influence of the southward IMF arrives at the ionosphere, the DP2 ionospheric convection is established (Figure 2c). One of the arcs that had remained at around 80 MLAT (Figure 2b) starts to move equatorward. This equatorward movement is also found in Figure 1. After a while, another arc appears at around 72 MLAT (Figure 2e), which is also found in Figure 1. These arcs move equatorward and finally appear to approach close to the quiet arc. The initial brightening occurs at around 69.5 min

京都大学 KYOTO UNIVERSITY
A Self-archived copy in
Kyoto University Research Information Repository
https://repository.kulib.kyoto-u.ac.jp
京都大学学術情報リポジトリ KURENAI 紅 Kyoto University Research Information Repository

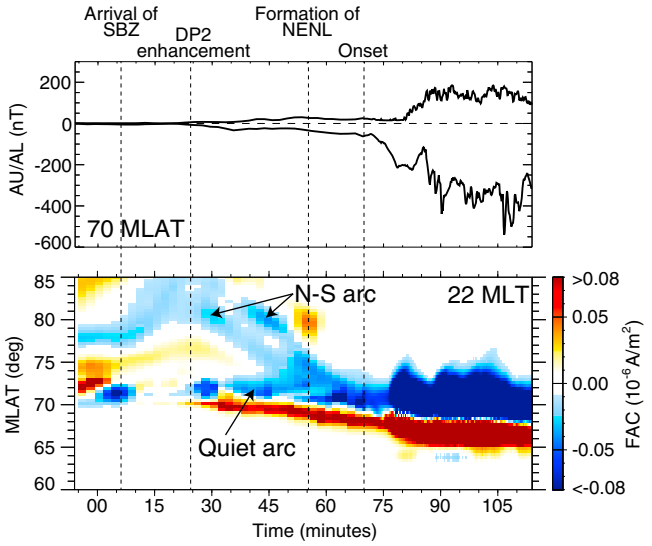

Figure 1. (top) *AU* and *AL* indices and (bottom) field-aligned current (negative upward) at 22 MLT as a function of MLAT and time.

(Figure 2g) and can be regarded as a full auroral breakup because the initial brightening is followed by a westward traveling surge (Paper 3).

To generalize the obtained feature, we continued the simulation. After a prolonged period of southward IMF, we turned it northward at $t = 120$ min. Then the arcs that are similar to those found in Figures 2a and 2b started to appear again (data now shown). Thus, we can believe that the simulation result may be held to be valid for the condition that IMF turns northward. Similar arcs are also found at high latitudes in the simulation result presented by *Ge et al.* [2011, Figure 11]. The evolution of the quiet arcs and the N-S arcs (shown in Figures 1 and 2) seems to resemble those observed in the growth phase [*Brittnacher et al.*, 1999; *Kepko et al.*, 2009; *Nishimura et al.*, 2010, 2011; *Mende et al.*, 2011].

3.2. Magnetospheric Origin of the Arcs

We focused on the three arcs labeled Arcs 1, 2, and 3 in Figure 2f and investigated their magnetospheric counterpart. Arcs 1 and 2 may be regarded as N-S arcs [*Nishimura et al.*, 2010], while Arc 3 may be considered a quiet arc [*Akasofu*, 1964] or a growth phase arc [*Nishimura et al.*, 2010]. Their latitudinal motion is identified in Figure 1. Figure 3 shows a bird's eye view of the current lines (yellow) and the magnetic field lines (white) extending from Arcs 1, 2, and 3. Three panels, which are normal to the X direction and placed at $X = -7$ *Re*, are inserted to show the plasma pressure (Figure 3a) and the parallel current density $J_{||}$ (Figures 3b and 3c). In Figures 3b and 3c, the blue (red) color indicates the current that is antiparallel (parallel) to the magnetic field, which is the upward (downward) current in the Northern Hemisphere. There are some features to be noted:

1. The current lines indicated in yellow are diverted from the magnetic field lines indicated in white. The diversion is caused by the diamagnetic (perpendicular) current.
2. The current lines pass through the region in which the plasma pressure and $J_{||}$ are structured.
3. The structured high-pressure region extends from the plasma sheet to high latitudes.
4. Arcs 2 and 3 share the same upward current region at $X = -7$ *Re*. This may suggest that quiet arcs and N-S arcs are probably indistinguishable from one another in terms of their upward FAC generation region. Namely, some quiet arcs and N-S arcs may be homogeneous.
5. Arc 2 is on an open field line, whereas Arc 3 is on a closed field line (data not shown). The diamagnetic current diverts (or guides) the current line from the region of an open field line to the region of a closed field line.
6. The structured high-pressure region is elongated to the distant tail, but the current lines are diverted from magnetic field lines and confined in the near-Earth region (data now shown). It seems that the contribution from the structured high-pressure region in the distant tail is very limited because most of the FACs generated in the distant tail cannot reach the ionosphere. Thus, the structured high-pressure region closed to the Earth may provide a direct, efficient influence on the generation of the arcs.

Figure 4 shows the plasma pressure in the Y-Z plane at $X = -7$ *Re* (right column) and in the X-Z plane at $Y = -1.5$ *Re* (left column). A noticeable feature is that the distribution of plasma pressure is highly disturbed toward the high latitude in the lobe. Some of the shapes are mushroom-like (finger-like) in the Y-Z plane, which may imply a kind of instability as mentioned below. Some protuberances of the high-pressure region seem to extend from the plasma sheet to higher latitudes and evolve toward the positive Z and negative Y direction in the Northern Hemisphere (Figure 4b). The evolution of the high-pressure region is considered to be due to advection rather than compression of the ambient plasma (data not shown). After the southward

京都大学 KYOTO UNIVERSITY
A Self-archived copy in
Kyoto University Research Information Repository
https://repository.kulib.kyoto-u.ac.jp
京都大学学術情報リポジトリ KURENAI 紅 Kyoto University Research Information Repository

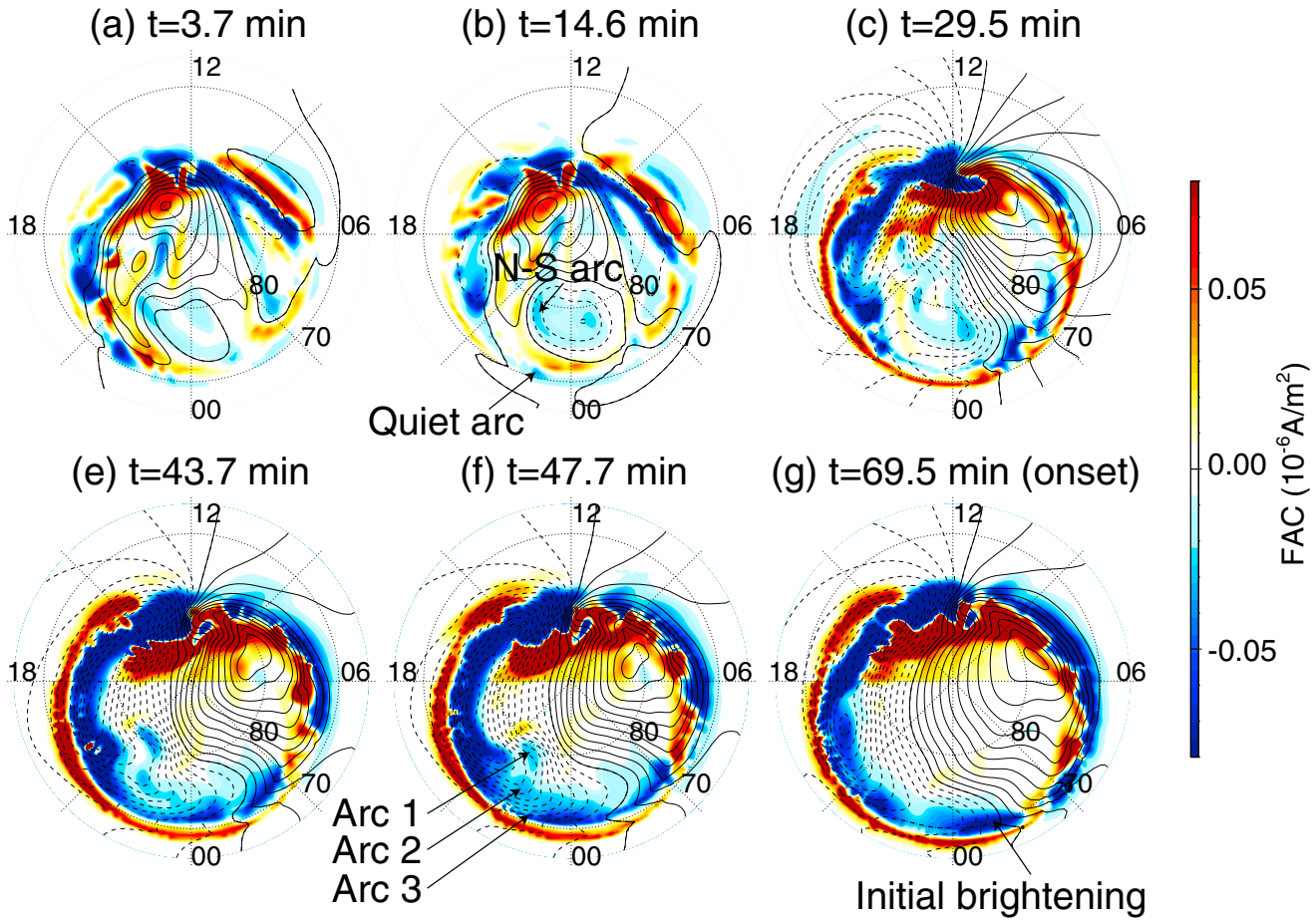

Figure 2. FAC at the ionosphere (negative upward). The contour line indicates the ionospheric electric potential at interval of 2 kV. The solid line indicates positive potential, and the dashed one indicates negative potential.

turning of IMF, the structured high-pressure region moves toward the plasma sheet as time progresses (Figures 4c and 4d). This region tends to lie in the *Y* direction as seen in the *Y-Z* plane with advancing time. Around $t = 55.7$ min, a NENL starts to form in the plasma sheet at $X \approx -42\,Re$ (Figure 4e), which releases magnetic tension. One of the high-latitude high-pressure regions coming from the lobe is found to approach the NENL but seems not to participate in the formation of the NENL for this particular simulation. As the consequence of the magnetic tension, an intense, localized high-pressure region suddenly appears near the outer edge of the plasma sheet at $t = 69.5$ min (Figure 4f) [*Birn et al.*, 2004; *Tanaka et al.*, 2010]. This localized high-pressure region generates localized upward currents. When this upward current is connected to the ionosphere, the initial brightening (sudden intensification of upward FAC) occurs (Papers 2 and 3).

Next, we focus on the generation of the structured high-pressure region at high latitude in the lobe. When perturbations begin within an initially uniform magnetic field, the generation of the FAC can be given by [*Paschmann et al.*, 2002]

$$\frac{\partial J_{||}}{\partial t} = \frac{1}{\mu_0}\mathbf{B}\cdot\nabla\Omega_{||}, \tag{1}$$

where $\Omega_{||} = \mathbf{B}\cdot(\nabla\times\mathbf{V})/B$, $\mathbf{B}$ is the magnetic field, and $\mathbf{V}$ is the velocity of the plasma. In the Northern Hemisphere, the upward current ($J_{||} < 0$) is generated when the parallel vorticity is larger at greater distances from the Earth along a field line. Figure 5 shows the plasma pressure, parallel vorticity $\Omega_{||}$, and the parallel current $J_{||}$ in the *Y-Z* plane at $X = -2.0$ Re and $t = 3.7$ min. A protuberance of the high-pressure region is found at high latitude (Figure 5a). The perpendicular flow velocity appears to look a negative *Y* and positive *Z* direction near the protuberance. The parallel vorticity is positive to the east of the protuberance and negative to the west of it (Figure 5b). The upward current flows through the eastward part of the protuberance, while the

京都大学 KYOTO UNIVERSITY
A Self-archived copy in
Kyoto University Research Information Repository
https://repository.kulib.kyoto-u.ac.jp
京都大学学術情報リポジトリ KURENAI 紅 Kyoto University Research Information Repository

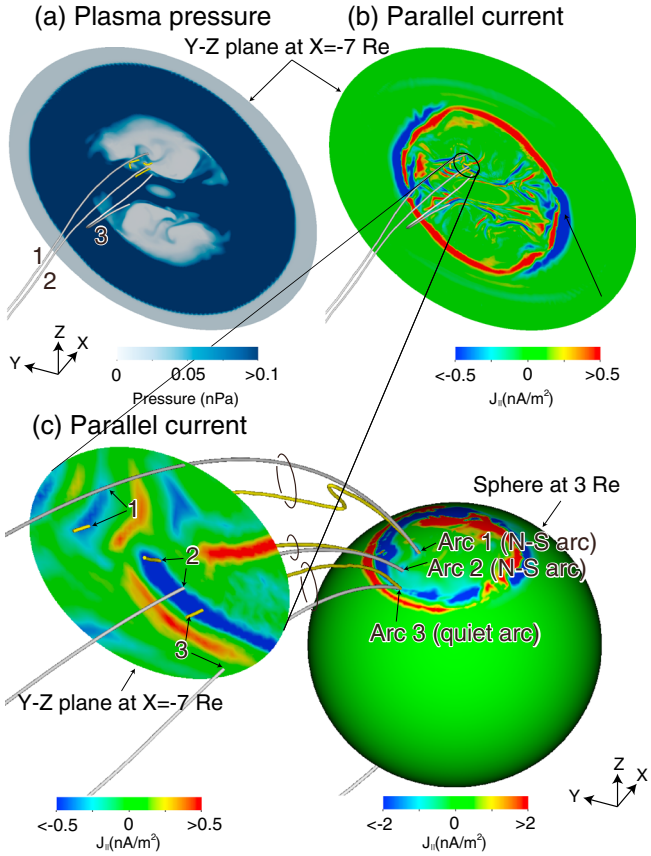

Figure 3. (a) Plasma pressure and (b and c) parallel current density in the *Y-Z* plane at $X = -7$ *Re*. In (c), parallel current is also drawn on the surface at 3 *Re*. The yellow and white lines indicate the current line and the magnetic field line, respectively, extending from Arcs 1, 2, and 3 at $t = 43.7$ min. The color codes indicate the parallel current density (negative upward in the Northern Hemisphere). We are looking down the Earth from the midnight-dawn sector in the Northern Hemisphere.

downward current through the westward part (Figure 5c). The polarity of this vorticity is consistent with that of $J_{||}$. The relationship between the parallel vorticity and the parallel current is also discussed in Paper 2.

In Figure 5d, a schematic drawing is present to show a possible mechanism for the formation of the structured high-pressure region. (1) A small disturbance in the magnetospheric plasma flow generates parallel vorticities that generate a pair of $J_{||}$. (2) $J_{||}$ is connected to the ionosphere. (3) In order to cancel out the space charge deposited by the FAC, an additional electric field (mostly eastward) is established in the ionosphere. (4) The redistributed electric field is transmitted to the magnetosphere as a shear Alfvén wave along a field line. (5) The eastward electric field pulls the plasma off the plasma sheet. The amplitude of the disturbance is enlarged. (6) As the high-pressure region moves, the ∇P force is not balanced by the Lorentz force, giving rise to the acceleration of plasma around it. (7) The vorticity generates or maintains a pair of $J_{||}$. The disturbance in the ionospheric electric potential identified around the FAC (Figure 2a) is consistent with this mechanism. This instability tends to works efficiently when the background convection electric field is weak, and the current line is almost parallel to the magnetic field line (Figure 3c). The near-Earth region (low altitude) under a northward IMF may preferentially satisfy this condition. The development of the high-pressure region presented here is not similar to the twisting of the plasma sheet, called cross-tail S [e.g., *White et al*., 1998; *Tanaka et al*., 2004]. This configuration of electric field, plasma pressure, and $J_{||}$ may favor an interchange-like instability between the magnetosphere and the ionosphere [*Sazykin et al*., 2002; *Ebihara et al*., 2005].

3.3. Attack Angle of Arcs

In order to explain the reason why the arcs tend to lie in the longitudinal direction under the southward IMF (growth phase), we present Figure 6 that shows the FAC and the north-south component of the ionospheric plasma flow at $t = 43.7$ min. Arcs 1, 2, and 3 are found in Figures 2a–2c and 3a and 3b. Arc 1 tends to lie along the equipotential line, whereas Arc 2 is skewed counterclockwise from the equipotential line. These features may be consistent with those found by *Nishimura et al*. [2010]. The skew or rotation of the arc may be accounted for by the gradient of the equatorward convection flow velocity [*Kadokura et al*., 2002]. The equatorward component of the convective flow is fast at high latitudes but becomes slower near the convection reversal (Figure 6b), due to the change in direction of the convection flow velocity. The gradient of the equatorward component of the flow would make the arcs align with the *Y* direction. The slowdown in the equatorward motion of the arcs has been also noted by *Brittnacher et al*. [1999] and *Friedrich et al*. [2001].

京都大学 KYOTO UNIVERSITY
A Self-archived copy in
Kyoto University Research Information Repository
https://repository.kulib.kyoto-u.ac.jp
京都大学学術情報リポジトリ KURENAI 紅 Kyoto University Research Information Repository

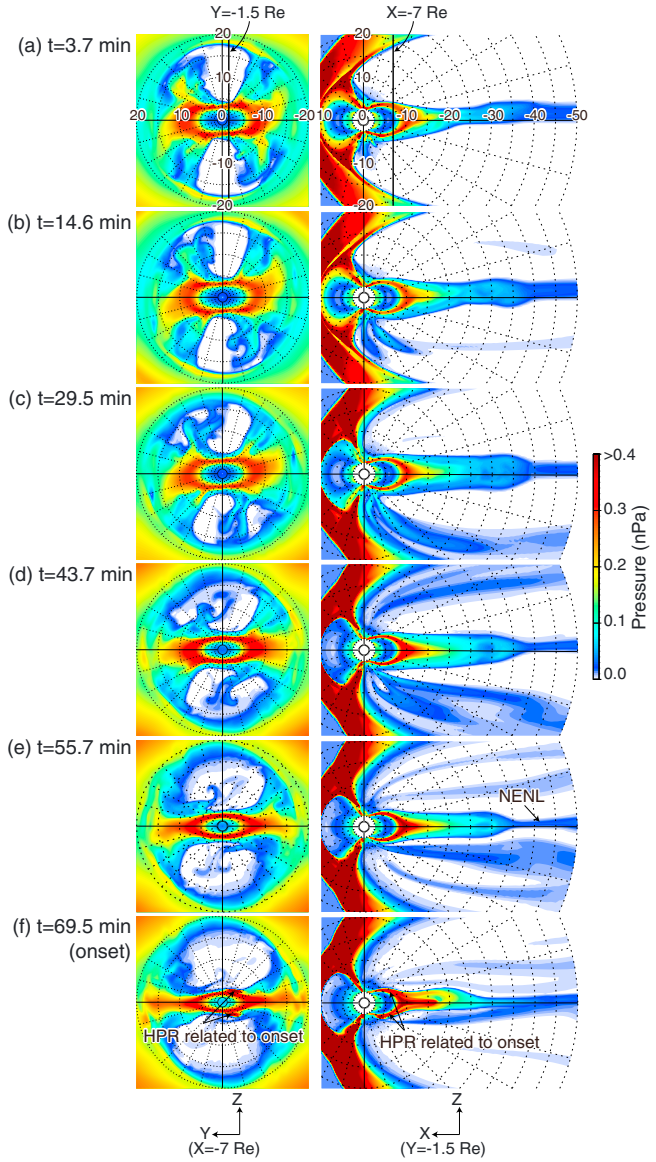

Figure 4. Plasma pressure in the *Y-Z* plane at (right column) $X = -7.0$ *Re*, and in the *X-Z* plane at (left column) $Y = -1.5$ *Re* (Re) at (a) 3.7, (b) 14.6, (c) 29.5, (d) 43.7, (e) 55.7, and (f) 69.5 min.

4. Discussion

4.1. Structure and Dynamics of Arcs

Nishimura et al. [2010] showed that N-S arcs are not always aligned with geomagnetic north. The angle between the N-S arc and geomagnetic north can range from −90° to 90°, and sometimes, the angle can change over the course of equatorward propagation. The arc can also be bent. These observations can be reasonably explained by our simulation results, that is, the N-S arc may be a manifestation of the structured high-pressure region at high latitudes. The direction of the arc is determined by the high-pressure region, which is disturbed by interchange-like instability. If the structured high-pressure region is insufficiently developed before the growth phase starts (e.g., relatively short duration of northward IMF), the quiet and N-S arcs will be almost absent.

In the simulation, the N-S arc moves equatorward when IMF is southward. In the course of equatorward moving, the magnitude of the upward FAC is tentatively intensified (Figure 1, $t \approx 30$ and ≈ 45 min) before the formation of the NENL ($t \approx 56$ min). This feature may resemble the "poleward boundary intensification"

京都大学 KYOTO UNIVERSITY
A Self-archived copy in
Kyoto University Research Information Repository
https://repository.kulib.kyoto-u.ac.jp
京都大学学術情報リポジトリ KURENAI 紅 Kyoto University Research Information Repository

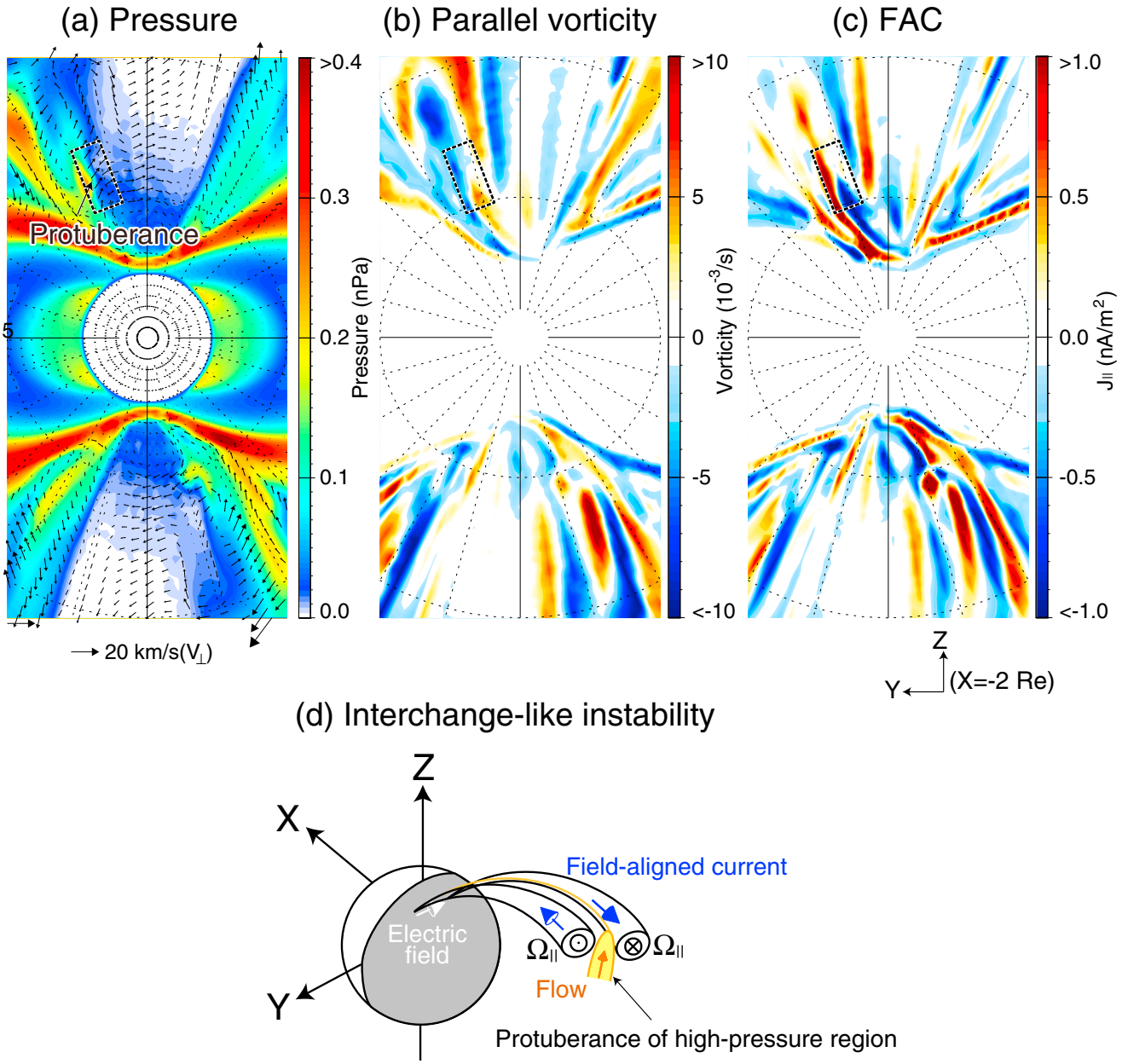

Figure 5. (a) Plasma pressure, (b) parallel vorticity $\Omega_{||}$, and (c) parallel current density $J_{||}$ (negative upward in the Northern Hemisphere) in the *Y*-*Z* plane at $X = -2.0$ Re at $t = 3.7$ min. The arrow indicates the plasma flow velocity perpendicular to the magnetic field. (d) A schematic drawing is present to explain the possible instability taking place in the coupling between the magnetosphere and the ionosphere.

(PBI) called by *Nishimura et al.* [2010, 2011] who attributed a tentative intensification of auroral brightness to an ionospheric manifestation of reconnection taking place in the plasma sheet. If the N-S arc is a manifestation of the high-pressure region at high latitudes, the PBI called by *Nishimura et al.* [2010, 2011] will be unnecessary to be associated with the reconnection. Originally, the term PBI has been introduced to indicate the initiation of auroral streamers that are found after the onset of auroral breakup and attributed to earthward fast flow in the plasma sheet [*Lyons et al.*, 1998, 1999, 2000; *Zesta et al.*, 2000, 2002, 2006; *Akasofu*, 2015].

An equatorward moving diffuse patch of aurora at 630.0 nm was also observed at the eastward of the N-S arcs [*Kepko et al.*, 2009]. Although the cause of the diffuse patch of aurora is unclear in the simulation, there is a possibility that the precipitating electrons that cause the diffuse patch may manifest the structured high-pressure

京都大学 KYOTO UNIVERSITY
A Self-archived copy in
Kyoto University Research Information Repository
https://repository.kulib.kyoto-u.ac.jp
京都大学学術情報リポジトリ KURENAI 紅 Kyoto University Research Information Repository

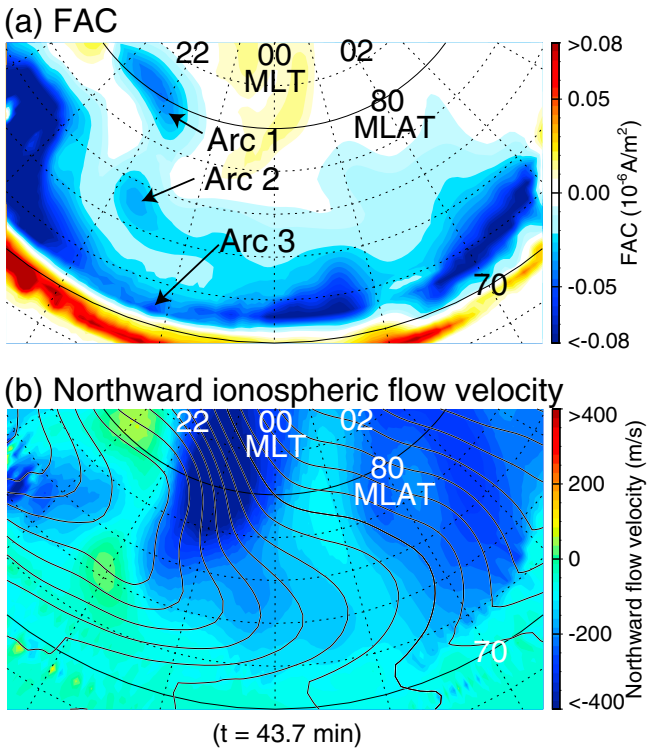

Figure 6. (a) FAC at the ionosphere (negative upward) and (b) north-south component of the ionospheric flow velocity at $t = 43.7$ min. The contour line indicates the ionospheric electric potential at interval of 2 kV.

region at high latitudes. The precipitating electrons move earthward along a field line, whereas the current line deviates from the field line due to the perpendicular current. Thus, the N-S arc can be displaced from diffuse patch of aurora.

4.2. Relationship With Onset

In the present simulation, the initial brightening takes place at $t = 69.5$ min, followed by the formation of bulge and WTS. The sequence that leads to the initial brightening and WTS is briefly summarized as follows. Readers may refer Paper 2 and Paper 3 for detailed description for the formation of the initial brightening and WTS. When IMF is southward, a near-Earth neutral line forms in the plasma sheet, which releases magnetic tension to compress plasma and accelerate plasma earthward. Due to slow mode variation, plasma pressure starts to increase along a field line, which coexists with flow vorticities generating strong FACs. When the FACs are connected to the ionosphere, initial brightening (sudden intensification of the upward FAC) takes place. As the earthward plasma flow continues, the plasma pressure increases at earlier and later MLTs. The ionospheric conductivity is enhanced in the upward FAC region. Because of the gradient of the conductivity, the ionospheric Hall current overflows. The convergence of the Hall current gives rise to the divergent electric field. The magnetospheric plasma moves counterclockwise at low-altitude magnetosphere (when viewed along a magnetic field line). The additional flow vorticity of the magnetospheric plasma generates a localized upward FAC, which may manifest WTS. The present result shows that the structured high-pressure region (associated with the quiet and N-S arcs) seems not to participate in the formation of the NENL (Figure 4e). That may mean that the structured high-pressure region (associated with the quiet and N-S arcs) is not a necessary condition for the formation of the NENL. Of course, there is a possibility that the structured high-pressure region (associated with the quiet and N-S arcs) merges with the plasma sheet and participates in the formation of the NENL. This would happen after a prolonged growth phase in which the structured high-pressure region could reach the plasma sheet before the formation of the NENL. Further investigation is required to confirm the overall role of the off-equatorial high-pressure region in the formation of the NENL.

Appearance of the quiet and N-S arcs is thought to be a manifestation of the magnetospheric processes that modify the M-I system and lead to the onset. *Akasofu* [1964] noted that longitudinally elongated quiet arcs move equatorward before onset and that one of the quiet arcs begins to show a sudden brightening. From an observational point of view, the onset arc and the other quiet arcs are essentially indistinguishable until the onset occurs. The simulation results also suggest that they are indistinguishable because the processes driving the development of the quiet arcs and those triggering the onset occur independently. The quiet arcs are associated with processes taking place at high latitudes, while the initial brightening is linked to processes taking place in the plasma sheet. Based on observations, it has been considered that both the quiet arcs and the onset arc are projected to the inner plasma sheet inside $X \sim -10\ Re$ along a magnetic field line [*Samson et al.*, 1992; *Donovan et al.*, 2008]. The projected locations of the arcs have been paid great attention to test competing models, such as "outside-in" [*Baker et al.*, 1996] and "inside-out" [*Lui*, 1996] models.

京都大学 KYOTO UNIVERSITY
A Self-archived copy in
Kyoto University Research Information Repository
https://repository.kulib.kyoto-u.ac.jp
京都大学学術情報リポジトリ KURENAI 紅 Kyoto University Research Information Repository

Lui et al. [2008] showed a substorm event in which an equatorward arc expanded at onset, whereas poleward arcs remained undisturbed. This observational fact would agree with the inside-out model if all the arcs were projected into the equatorial plane farther downtail of the region where an onset triggering process (local instability) takes place. In the inside-out model, the onset triggering process may disturb the most equatorward arc, and the remnant of the arcs may remain undisturbed. If one thinks that a large part of the N-S arcs is projected into the equatorial plane, one will expect a thick plasma sheet [*Mende et al*., 2011, Figure 11]. This may be inconsistent with previous thoughts in which the plasma sheet is so thin during the growth phase [e.g., *Pulkkinen*, 1991; *Pritchett and Coroniti*, 1995, 1997; *Pulkkinen et al*., 1991, 1994; *Hesse et al*., 1996; *Kubyshkina et al*., 2011, Paper 1]. Contrarily, the present study suggests that the quiet and N-S arcs will be unnecessarily projected into the equatorial plane along a magnetic field line. The upward FACs that are related to the arcs are not always aligned with magnetic field lines because of the presence of the perpendicular current (Figure 3). The current lines extending from the quiet and N-S arcs are confined in the near-Earth region (at low altitudes). Thus, it may be said that the quiet and N-S arcs are a manifestation of the magnetospheric processes taking place at low altitudes and at high latitudes in the near-Earth region. If so, a thick plasma sheet will be no longer required to explain the formation of the N-S arcs. Paper 1 shows a relatively homogeneous quiet arc in comparison with that presented in this paper. As explained in Paper 1, such a quiet arc can also be formed by large-scale convection shear in the transition region between the plasma sheet and the lobe. During the growth phase, the large-scale convection stagnates inside the plasma sheet due to a weak coupling with the ionospheric convection because of a topological mismatch [*Tanaka et al*., 2010]. The upward FAC associated with such a quiet arc occurs to transmit the shear motion from the magnetosphere to the ionosphere. Consequently, the shear motion excites quiet arcs. In both cases, the quiet arcs may be understood to the global context. Traditionally, the upward FAC that coexists with the quiet arc is understood rather locally. They are attributed to the particle precipitation due to pitch angle scattering in a curved magnetic field lines or wave particle interaction [*Sergeev et al*., 2011]. Since the MHD simulation cannot deal with the particle precipitation explicitly, further investigations are required to confirm it.

The undisturbed poleward arcs at the onset may be explained by our simulation results. The quiet and N-S arcs are related to the processes taking place at high latitudes (i.e., structured high-pressure region moving in the latitudinal direction), whereas the initial brightening and the subsequent poleward expansion of aurora are related to the processes confined to the lower latitude region (i.e., high-pressure region moving in the radial direction in the plasma sheet) (Figure 4). The initial brightening is initiated by the formation of NENL (Papers 2 and 3) in our simulation, which is similar to the so-called outside-in model [*Baker et al*., 1996]. If one assumes that auroral structures can be mapped along a magnetic field line into the equatorial plane, the outside-in model will fail to explain fully the undisturbed poleward arcs. It is again emphasized that a simple projection from the ionosphere to the equatorial plane along a magnetic field line may cause confusion and misunderstanding because a substorm progresses in the three-dimensional space.

As shown hitherto, the simulation results in this paper indicate that the N-S arc is probably not a direct precursor of the onset. This result is quite different from estimations based on observations [*Kepko et al*., 2004; *Nishimura et al*., 2010, 2011; *Lyons et al*., 2010]. The simulation results also indicate that the sudden intensification of the upward FAC at onset is attributed to the sudden formation of the high-pressure region at high latitudes (Papers 2 and 3). Traditionally, the sudden intensification of the upward FAC is attributed to the formation of the SCW due to instabilities or additional flow vorticities taking place near the equatorial plane. The SCW that connects the ionosphere to the cross-tail current is not found in the simulation (Paper 2). The reason is that the current line extending from the initial brightening is diverted from a magnetic field line. The current line tends to connect to the cusp-mantle dynamo. The sudden change of the magnetospheric system that characterizes the onset comes from the state transition through the change in the global force balance [*Tanaka et al*., 2010]. This process results in the sudden formation of the high-pressure region at high latitudes in the near-Earth region (Papers 1, 2, and 3).

4.3. Structured High-Pressure Region

Further in situ observations are needed to confirm the existence of this structured high-pressure region and its association with the auroral forms that appear before the onset of auroral substorm expansion. The simulation result suggests that the structured high-pressure region is elongated poleward (away from the equatorial plane) from the prime plasma sheet because of the consequence of the M-I coupling. *Shi et al*. [2013]

京都大学 KYOTO UNIVERSITY
A Self-archived copy in
Kyoto University Research Information Repository
https://repository.kulib.kyoto-u.ac.jp
京都大学学術情報リポジトリ KURENAI 紅 Kyoto University Research Information Repository

found localized regions of high-density ions in the lobe. The pitch angle distribution of the ions is almost isotropic, and the characteristic energy is ~keV. Most of the high-density regions are observed when IMF looks northward. *Shi et al*. [2013] claimed that the localized high-density regions in the lobe are a manifestation of direct entry of the solar wind plasma. There may be possibility that the localized high-density regions are the structured high-pressure regions elongated from the main body of the plasma sheet as shown in Figure 4.

5. Conclusions

The major conclusions from this study can be summarized as follows:

1. When the convection electric field is weak, such as in a northward IMF, the plasma pressure is highly structured as a result of interchange-like instability in the high-latitude magnetosphere. The structured high-pressure region tends to be elongated away from the plasma sheet toward high latitudes.
2. When the convection electric field is enhanced, such as in a southward IMF, the structured high-pressure region moves toward the plasma sheet, together with the upward FAC region. This can be observed as elongated arcs, including both quiet arcs and N-S arcs, moving equatorward in the ionosphere. The direction of the arc depends on the structure of the high-pressure region and can be skewed or bent over the course of equatorward propagation. Over the course of the equatorward propagation, the upward field-aligned current is tentatively intensified before the formation of the near-Earth neutral line. This probably means that poleward boundary intensifications (PBIs) are not necessarily attributed to the formation of a near-Earth neutral line.
3. Because the current line is diverted from the magnetic field line by the diamagnetic current, the movement of the arcs does not always reflect the movement of the structured high-pressure region. Because of the existence of the diamagnetic current, the current line can travel from the region of an open field line to the region of a closed field line.
4. The generation mechanism for the initial brightening (Paper 2) and WTS (Paper 3) seems not to disturb the structured high-pressure regions that remain in the high-latitude magnetosphere. This may explain the observational fact that quiet arcs are typically undisturbed, with the exception of the onset arc, during auroral breakup [*Akasofu*, 1964; *Lui et al*., 2008].

Acknowledgments
We thank Takashi Kikuchi for fruitful comments and discussion. The computer simulation was performed on the KDK computer system at the Research Institute for Sustainable Humanosphere (RISH), Kyoto University. This study was supported by JSPS KAKENHI grants 15H03732 and 15H05815. The simulation data are available upon request.

References

Akasofu, S.-I. (1964), The development of the auroral substorm, *Planet. Space Sci.*, *12*, 273–282.
Akasofu, S.-I. (2015), Auroral substorms as an electrical discharge phenomenon, *Prog. Earth Planet Sci.*, *2*, 20, doi:10.1186/s40645-015-0050-9.
Akasofu, S.-I., and A. L. Snyder (1972), Comments on the growth phase of magnetospheric substorms, *J. Geophys. Res.*, *77*(31), 6275–6277, doi:10.1029/JA077i031p06275.
Antonova, E. E. (1993), The development of initial substorm expansion phase disturbance due to generation of localized electric fields in the region of maximum upward field-aligned current, *Adv. Space Res.*, *13*(4), 261–264.
Atkinson, G. (1970), Auroral arcs: Result of the interaction of a dynamic magnetosphere with the ionosphere, *J. Geophys. Res.*, *75*(25), 4746–4755, doi:10.1029/JA075i025p04746.
Baker, D. N., T. I. Pulkkinen, V. Angelopoulos, W. Baumjohann, and R. L. McPherron (1996), Neutral line model of substorms: Past results and present view, *J. Geophys. Res.*, *101*(A6), 12,975–13,010, doi:10.1029/95JA03753.
Birn, J., and M. Hesse (1996), Details of current disruption and diversion in simulations of magnetotail dynamics, *J. Geophys. Res.*, *101*(A7), 15,345–15,358, doi:10.1029/96JA00887.
Birn, J., M. Hesse, G. Haerendel, W. Baumjohann, and K. Shiokawa (1999), Flow braking and the substorm current wedge, *J. Geophys. Res.*, *104*(A9), 19,895–19,903, doi:10.1029/1999JA900173.
Birn, J. M., J. Raeder, Y. L. Wang, R. A. Wolf, and M. Hesse (2004), On the propagation of bubbles in the magnetotail, *Ann. Geophys.*, *22*, 1773–1786.
Brittnacher, M., M. Fillingim, G. Parks, G. Germany, and J. Spann (1999), Polar cap area and boundary motion during substorms, *J. Geophys. Res.*, *104*(A6), 12,251–12,262, doi:10.1029/1998JA900097.
Chen, C. X., and R. A. Wolf (1999), Theory of thin-filament motion in Earth's magnetotail and its application to bursty bulk flows, *J. Geophys. Res.*, *104*(A7), 14,613–14,626, doi:10.1029/1999JA900005.
Coroniti, F. V., and P. L. Pritchett (2014), The quiet evening auroral arc and the structure of the growth phase near-Earth plasma sheet, *J. Geophys. Res. Space Physics*, *119*, 1827–1836, doi:10.1002/2013JA019435.
Davis, T. N. (1962), The morphology of the auroral displays of 1957–1958: 2. Detail analyses of Alaska data and analyses of high-latitude data, *J. Geophys. Res.*, *67*(1), 75–110, doi:10.1029/JZ067i001p00075.
de la Beaujardière, O., L. R. Lyons, J. M. Ruohoniemi, E. Friis-Christensen, C. Danielsen, F. J. Rich, and P. T. Newell (1994), Quiet-time intensifications along the poleward auroral boundary near midnight, *J. Geophys. Res.*, *99*(A1), 287, doi:10.1029/93JA01947.
Donovan, E., et al. (2008), Simultaneous THEMIS in situ and auroral observations of a small substorm, *Geophys. Res. Lett.*, *35* L17S18, doi:10.1029/2008GL033794.
Ebihara, Y., and T. Tanaka (2015a), Substorm simulation: Insight into the mechanisms of initial brightening, *J. Geophys. Res. Space Physics*, *120*, 7270–7288, doi:10.1002/2015JA021516.
Ebihara, Y., and T. Tanaka (2015b), Substorm simulation: Formation of westward traveling surge, *J. Geophys. Res. Space Physics*, *120*, doi:10.1002/2015JA021697.

京都大学 KYOTO UNIVERSITY
A Self-archived copy in
Kyoto University Research Information Repository
https://repository.kulib.kyoto-u.ac.jp
京都大学学術情報リポジトリ KURENAI 紅 Kyoto University Research Information Repository

Ebihara, Y., M.-C. Fok, S. Sazykin, M. F. Thomsen, M. R. Hairston, D. S. Evans, F. J. Rich, and M. Ejiri (2005), Ring current and the magnetosphere-ionosphere coupling during the superstorm of 20 November 2003, *J. Geophys. Res.*, *110*, A09S22, doi:10.1029/2004JA010924.

Ebihara, Y., T. Tanaka, and T. Kikuchi (2014), Counter equatorial electrojet and overshielding after substorm onset: Global MHD simulation study, *J. Geophys. Res. Space Physics*, *119*, 7281–7296, doi:10.1002/2014JA020065.

Echim, M. M., R. Maggiolo, M. Roth, and J. De Keyser (2009), A magnetospheric generator driving ion and electron acceleration and electric currents in a discrete auroral arc observed by Cluster and DMSP, *Geophys. Res. Lett.*, *36*, L12111, doi:10.1029/2009GL038343.

Eliasson, L., R. Lundin, and J. S. Murphree (1987), Polar cap arcs observed by the Viking satellite, *Geophys. Res.*, *14*, 451–454.

Friedrich, E., J. C. Samson, I. Voronkov, and G. Rostoker (2001), Dynamics of the substorm expansive phase, *J. Geophys. Res.*, *106*, 13,145–13,163, doi:10.1029/2000JA000292.

Galperin, Y. I., and J. M. Bosqued (1999), Stationary magnetospheric convection on November 24, 1981. 1. A case study of "pressure-gradient/minimum-B" auroral arc generation, *Ann. Geophys.*, *17*, 358–374.

Galperin, Y. I., A. V. Volosevich, and L. M. Zelenyi (1992), Pressure gradient structures in the tail neutral sheet as "roots of the arc" with some effects of stochasticity, *Geophys. Res. Lett.*, *19*(21), 2163–2166, doi:10.1029/92GL02178.

Ge, Y. S., J. Raeder, V. Angelopoulos, M. L. Gilson, and A. Runov (2011), Interaction of dipolarization fronts within multiple bursty bulk flows in global MHD simulations of a substorm on 27 February 2009, *J. Geophys. Res.*, *116*, A00I23, doi:10.1029/2010JA015758.

Haerendel, G. (2007), Auroral arcs as sites of magnetic stress release, *J. Geophys. Res.*, *112*, A09214, doi:10.1029/2007JA012378.

Haerendel, G. (2010), Equatorward moving arcs and substorm onset, *J. Geophys. Res.*, *115*, A07212, doi:10.1029/2009JA015117.

Haerendel, G., H. U. Frey, C. C. Chaston, O. Amm, L. Juusola, R. Nakamura, E. Seran, and J. M. Weygand (2012), Birth and life of auroral arcs embedded in the evening auroral oval convection: A critical comparison of observations with theory, *J. Geophys. Res.*, *117*, A12220, doi:10.1029/2012JA018128.

Hamrin, M., et al. (2006), Observations of concentrated generator regions in the nightside magnetosphere by Cluster/FAST conjunctions, *Ann. Geophys.*, *24*, 637–649, doi:10.5194/angeo-24-637-2006.

Hasegawa, H., N. Ohno, and T. Sato (2010), Simulation of feedback instability in the coupled magnetosphere-ionosphere system, *J. Geophys. Res.*, *115*, A08304, doi:10.1029/2009JA015093.

Henderson, M. G., G. D. Reeves, and J. S. Murphree (1998), Are north-south structures an ionospheric manifestation of bursty bulk flows?, *Geophys. Res. Lett.*, *25*, 3737–3740, doi:10.1029/98GL02692.

Hesse, M., and J. Birn (1994), MHD modeling of magnetotail instability for localized resistivity, *J. Geophys. Res.*, *99*(A5), 8565–8576, doi:10.1029/94JA00441.

Hesse, M., D. Winske, M. Kuznetsova, J. Birn, and K. Schindler (1996), Hybrid modeling of the formation of thin current sheets in magnetotail configurations, *J. Geomagn. Geoelectr.*, *48*, 749–763.

Hoffman, R. A., and J. L. Burch (1973), Electron precipitation patterns and substorm morphology, *J. Geophys. Res.*, *78*(16), 2867–2884, doi:10.1029/JA078i016p02867.

Ismail, S., and C.-I. Meng (1982), A classification of polar cap auroral arcs, *Planet. Space Sci.*, *30*, 319–330.

Ismail, S., D. D. Wallis, and L. L. Cogger (1977), Characteristics of polar cap Sun-aligned arcs, *J. Geophys. Res.*, *82*(29), 4741–4749, doi:10.1029/JA082i029p04741.

Jiang, F., R. J. Strangeway, M. G. Kivelson, J. M. Weygand, R. J. Walker, K. K. Khurana, Y. Nishimura, V. Angelopoulos, and E. Donovan (2012), In situ observations of the "preexisting auroral arc" by THEMIS all sky imagers and the FAST spacecraft, *J. Geophys. Res.*, *117*, A05211, doi:10.1029/2011JA017128.

Jiang, F., M. G. Kivelson, R. J. Strangeway, K. K. Khurana, and R. Walker (2015), Ionospheric flow shear associated with the preexisting auroral arc: A statistical study from the FAST spacecraft data, *J. Geophys. Res. Space Physics*, *120*, 5194–5213, doi:10.1002/2013JA019255.

Johnson, M. L., J. S. Murphree, G. T. Marklund, and T. Karlsson (1998), Progress on relating optical auroral forms and electric field patterns, *J. Geophys. Res.*, *103*(A3), 4271–4284, doi:10.1029/97JA00854.

Kadokura, A., A.-S. Yukimatu, M. Ejiri, T. Oguti, M. Pinnock, and M. R. Hairston (2002), Detailed analysis of a substorm event on 6 and 7 June 1989. 1. Growth phase evolution of nightside auroral activities and ionospheric convection toward expansion phase onset, *J. Geophys. Res.*, *107*(A12), 1479, doi:10.1029/2001JA009127.

Kamide, Y. (1974), Association of DP and DR fields with the interplanetary magnetic field variation, *J. Geophys. Res.*, *79*(1), 49–55, doi:10.1029/JA079i001p00049.

Kamide, Y., and S. Matsushita (1978), A unified view of substorm sequences, *J. Geophys. Res.*, *83*(A5), 2103–2108, doi:10.1029/JA083iA05p02103.

Keiling, A., et al. (2009), Substorm current wedge driven by plasma flow vortices: THEMIS observations, *J. Geophys. Res.*, *114*, A00C22, doi:10.1029/2009JA014114.

Kepko, L., M. G. Kivelson, and R. L. McPherron (2004), Relative timing of substorm onset phenomena, *J. Geophys. Res.*, *109*, A04203, doi:10.1029/2003JA010285.

Kepko, L., E. Spanswick, V. Angelopoulos, E. Donovan, J. McFadden, K.-H. Glassmeier, J. Raeder, and H. J. Singer (2009), Equatorward moving auroral signatures of a flow burst observed prior to auroral onset, *Geophys. Res. Lett.*, *36*, L24104, doi:10.1029/2009GL041476.

Kepko, L., R. L. McPherron, O. Amm, S. Apatenkov, W. Baumjohann, J. Birn, M. Lester, R. Nakamura, T. I. Pulkkinen, and V. Sergeev (2014), Substorm current wedge revisited, *Space Sci. Rev.*, *190*, 1–46, doi:10.1007/s11214-014-0124-9.

Kokubun, S. (1971), Polar substorm and interplanetary magnetic field, *Planet. Space Sci.*, *19*, 697–704, doi:10.1016/0032-0633(71)90028-6.

Korth, H., Y. Zhang, B. J. Anderson, T. Sotirelis, and C. L. Waters (2014), Statistical relationship between large-scale upward field-aligned currents and electron precipitation, *J. Geophys. Res. Space Physics*, *119*, 6715–6731, doi:10.1002/2014JA019961.

Kubyshkina, M., V. Sergeev, N. Tsyganenko, V. Angelopoulos, A. Runov, E. Donovan, H. Singer, U. Auster, and W. Baumjohann (2011), Time-dependent magnetospheric configuration and breakup mapping during a substorm, *J. Geophys. Res.*, *116*, A00I27, doi:10.1029/2010JA015882.

Lassen, K., and C. Danielsen (1978), Quiet time pattern of auroral arcs for different directions of the interplanetary magnetic field in the Y-Z plane, *J. Geophys. Res.*, *83*(A11), 5277–5284, doi:10.1029/JA083iA11p05277.

Lassen, K., J. R. Sharber, and J. D. Winningham (1977), The development of auroral and geomagnetic substorm activity after a southward turning of the interplanetary magnetic field following several hours of magnetic calm, *J. Geophys. Res.*, *82*(32), 5031–5050, doi:10.1029/JA082i032p05031.

Lessard, M. R., W. Lotko, J. LaBelle, W. Peria, C. W. Carlson, F. Creutzberg, and D. D. Wallis (2007), Ground and satellite observations of the evolution of growth phase auroral arcs, *J. Geophys. Res.*, *112*, A09304, doi:10.1029/2006JA011794.

Lotko, W., A. V. Streltsov, and C. W. Carlson (1998), Discrete auroral arc, electrostatic shock and suprathermal electrons powered by dispersive, anomalously resistive field line resonance, *Geophys. Res. Lett.*, *25*(24), 4449–4452, doi:10.1029/1998GL900200.

京都大学 KYOTO UNIVERSITY
A Self-archived copy in
Kyoto University Research Information Repository
https://repository.kulib.kyoto-u.ac.jp
京都大学学術情報リポジトリ KURENAI 紅 Kyoto University Research Information Repository

Lui, A. T. Y. (1996), Current disruption in the Earth's magnetosphere: Observations and models, *J. Geophys. Res.*, *101*(A6), 13,067–13,088, doi:10.1029/96JA00079.
Lui, A. T. Y., et al. (2008), Determination of the substorm initiation region from a major conjunction interval of THEMIS satellites, *J. Geophys. Res.*, *113*, A00C04, doi:10.1029/2008JA013424.
Lyon, J. G., R. E. Lopez, C. C. Goodrich, M. Wiltberger, and K. Papadopoulos (1998), Simulation of the March 9, 1995, substorm: Auroral brightening and the onset of lobe reconnection, *Geophys. Res. Lett.*, *25*(15), 3039–3042, doi:10.1029/98GL00662.
Lyons, L. (1980), Generation of large-scale regions of auroral currents, electric potentials, and precipitation by the divergence of the convection electric field, *J. Geophys. Res.*, *85*(A1), 17–24, doi:10.1029/JA085iA01p00017.
Lyons, L. R., and J. C. Samson (1992), Formation of the stable auroral arc that intensifies at substorm onset, *Geophys. Res. Lett.*, *19*(21), 2171–2174, doi:10.1029/92GL02494.
Lyons, L. R., G. T. Blanchard, J. C. Samson, J. M. Ruohoniemi, R. A. Greenwald, G. D. Reeves, and J. D. Scudder (1998), Near Earth plasma sheet penetration and geomagnetic disturbances, in *New Perspectives on the Earth's Magnetotail*, edited by A. Nishida et al., 241 pp., AGU, Washington, D. C.
Lyons, L. R., T. Nagai, G. T. Blanchard, J. C. Samson, T. Yamamoto, T. Mukai, A. Nishida, and S. Kokubun (1999), Association between GEOTAIL plasma flows and auroral poleward boundary intensifications observed by CANOPUS photometers, *J. Geophys. Res.*, *104*(A3), 4485–4500, doi:10.1029/1998JA900140.
Lyons, L. R., E. Zesta, J. C. Samson, and G. D. Reeves (2000), Auroral disturbances during the January 10, 1997 magnetic storm, *Geophys. Res. Lett.*, *27*(20), 3237–3240, doi:10.1029/1999GL000014.
Lyons, L. R., Y. Nishimura, Y. Shi, S. Zou, H.-J. Kim, V. Angelopoulos, C. Heinselman, M. J. Nicolls, and K.-H. Fornacon (2010), Substorm triggering by new plasma intrusion: Incoherent-scatter radar observations, *J. Geophys. Res.*, *115*, A07223, doi:10.1029/2009JA015168.
Lyons, L. R., Y. Nishimura, H.-J. Kim, E. Donovan, V. Angelopoulos, G. Sofko, M. Nicolls, C. Heinselman, J. M. Ruohoniemi, and N. Nishitani (2011), Possible connection of polar cap flows to pre- and post-substorm onset PBIs and streamers, *J. Geophys. Res.*, *116*, A12225, doi:10.1029/2011JA016850.
Lysak, R. L., and C. T. Dum (1983), Dynamics of magnetosphere-ionosphere coupling including turbulent transport, *J. Geophys. Res.*, *88*(A1), 365–380, doi:10.1029/JA088iA01p00365.
Lysak, R. L., and Y. Song (2002), Energetics of the ionospheric feedback instability, *J. Geophys. Res.*, *107*(A8), 1160, doi:10.1029/2001JA000308.
Marghitu, O., M. Hamrin, B. Klecker, K. Rönnmark, S. Buchert, L. M. Kistler, M. André, and H. Rème (2006), Experimental investigation of auroral generator regions with conjugate Cluster and FAST data, *Ann. Geophys.*, *24*, 619–635, doi:10.5194/angeo-24-619-2006.
Marklund, G. T. (1984), Auroral arc classification scheme based on the observed arc-associated electric field pattern, *Planet. Space Sci.*, *32*, 193–211.
McPherron, R. L. (1970), Growth phase of magnetospheric substorms, *J. Geophys. Res.*, *75*(28), 5592–5599, doi:10.1029/JA075i028p05592.
McPherron, R. L., C. T. Russell, and M. P. Aubry (1973), Satellite studies of magnetospheric substorms on August 15, 1968: 9. Phenomenological model for substorms, *J. Geophys. Res.*, *78*(16), 3131–3149, doi:10.1029/JA078i016p03131.
Mende, S. B., H. U. Frey, V. Angelopoulos, and Y. Nishimura (2011), Substorm triggering by poleward boundary intensification and related equatorward propagation, *J. Geophys. Res.*, *116*, A00I31, doi:10.1029/2010JA015733.
Meng, C.-I. (1976), Simultaneous observations of low-energy electron precipitation and optical auroral arcs in the evening sector by the DMSP 32 satellite, *J. Geophys. Res.*, *81*(16), 2771–2785, doi:10.1029/JA081i016p02771.
Moriguchi, T., A. Nakamizo, T. Tanaka, T. Obara, and H. Shimazu (2008), Current systems in the Jovian magnetosphere, *J. Geophys. Res.*, *113*, A05204, doi:10.1029/2007JA012751.
Mozer, F. S., and A. Hull (2001), Origin and geometry of upward parallel electric fields in the auroral acceleration region, *J. Geophys. Res.*, *106*(A4), 5763–5778, doi:10.1029/2000JA900117.
Nakamizo, A., T. Tanaka, Y. Kubo, S. Kamei, H. Shimazu, and H. Shinagawa (2009), Development of the 3-D MHD model of the solar corona-solar wind combining system, *J. Geophys. Res.*, *114*, A07109, doi:10.1029/2008JA013844.
Nakamura, R., W. Baumjohann, R. Schödel, M. Brittnacher, V. A. Sergeev, M. Kubyshkina, T. Mukai, and K. Liou (2001), Earthward flow bursts, auroral streamers, and small expansions, *J. Geophys. Res.*, *106*(A6), 10,791–10,802, doi:10.1029/2000JA000306.
Nakamura, R., et al. (2002), Motion of the dipolarization front during a flow burst event observed by Cluster, *Geophys. Res. Lett.*, *29*(20), 1942, doi:10.1029/2002GL015763.
Newell, P. T., D. Xu, C.-I. Meng, and M. G. Kivelson (1997), Dynamical polar cap: A unifying approach, *J. Geophys. Res.*, *102*(A1), 127–139, doi:10.1029/96JA03045.
Nishida, A. (1968), Coherence of geomagnetic DP 2 fluctuations with interplanetary magnetic variations, *J. Geophys. Res.*, *73*(17), 5549–5559, doi:10.1029/JA073i017p05549.
Nishimura, Y., L. Lyons, S. Zou, V. Angelopoulos, and S. Mende (2010), Substorm triggering by new plasma intrusion: THEMIS all-sky imager observations, *J. Geophys. Res.*, *115*, A07222, doi:10.1029/2009JA015166.
Nishimura, Y., L. R. Lyons, V. Angelopoulos, T. Kikuchi, S. Zou, and S. B. Mende (2011), Relations between multiple auroral streamers, pre-onset thin arc formation, and substorm auroral onset, *J. Geophys. Res.*, *116*, A09214, doi:10.1029/2011JA016768.
Nishimura, Y., L. R. Lyons, T. Kikuchi, V. Angelopoulos, E. F. Donovan, S. B. Mende, and H. Lühr (2012), Relation of substorm pre-onset arc to large-scale field-aligned current distribution, *Geophys. Res. Lett.*, *39*, L22101, doi:10.1029/2012GL053761.
Nishimura, Y., L. R. Lyons, X. Xing, V. Angelopoulos, E. F. Donovan, S. B. Mende, J. W. Bonnell, and U. Auster (2013), Tail reconnection region versus auroral activity inferred from conjugate ARTEMIS plasma sheet flow and auroral observations, *J. Geophys. Res. Space Physics*, *118*, 5758–5766, doi:10.1002/jgra.50549.
Ogawa, T., and T. Sato (1971), New mechanism of auroral arcs, *Planet. Space Sci.*, *19*(11), 1393–1412.
Oguti, T. (1973), Hydrogen emission and electron aurora at the onset of the auroral breakup, *J. Geophys. Res.*, *78*(31), 7543–7547, doi:10.1029/JA078i031p07543.
Ohtani, S., and J. Raeder (2004), Tail current surge: New insights from a global MHD simulation and comparison with satellite observations, *J. Geophys. Res.*, *109*, A01207, doi:10.1029/2002JA009750.
Palmroth, M., P. Janhunen, G. Germany, D. Lummerzheim, K. Liou, D. N. Baker, C. Barth, A. T. Weatherwax, and J. Watermann (2006), Precipitation and total power consumption in the ionosphere: Global MHD simulation results compared with Polar and SNOE observations, *Ann. Geophys.*, *24*, 861–872.
Paschmann, G., S. Haaland, and R. Treumann (Eds.) (2002), *Auroral Plasma Physics*, Kluwer Acad., Boston.
Pritchett, P. L., and F. V. Coroniti (1995), Formation of thin current sheets during plasma sheet convection, *J. Geophys. Res.*, *100*, 23,551–23,565, doi:10.1029/95JA02540.
Pritchett, P. L., and F. V. Coroniti (1997), Interchange and kink modes in the near-Earth plasma sheet and their associated plasma flows, *Geophys. Res. Lett.*, *24*, 2925–2928, doi:10.1029/97GL02950.

京都大学 KYOTO UNIVERSITY
A Self-archived copy in
Kyoto University Research Information Repository
https://repository.kulib.kyoto-u.ac.jp
京都大学学術情報リポジトリ KURENAI 紅 Kyoto University Research Information Repository

Pulkkinen, T. I. (1991), A study of magnetic field and current configurations in the magnetotail at time of a substorm onset, *Planet. Space Sci.*, *39*, 833–845, doi:10.1016/0032-0633(91)90088-R.
Pulkkinen, T. I., D. N. Baker, D. H. Fairfield, R. J. Pellinen, J. S. Murphree, R. D. Elphinstone, R. L. McPherron, J. F. Fennell, R. E. Lopez, and T. Nagai (1991), Modeling the growth phase of a substorm using the Tsyganenko model and multi-spacecraft observations: CDAW-9, *Geophys. Res. Lett.*, *18*(11), 1963–1966, doi:10.1029/91GL02002.
Pulkkinen, T. I., D. N. Baker, D. G. Mitchell, R. L. McPherron, C. Y. Huang, and L. A. Frank (1994), Thin current sheets in the magnetotail during substorms: CDAW 6 revisited, *J. Geophys. Res.*, *99*(A4), 5793–5803, doi:10.1029/93JA03234.
Raeder, J., R. L. McPherron, L. A. Frank, S. Kokubun, G. Lu, T. Mukai, W. R. Paterson, J. B. Sigwarth, H. J. Singer, and J. A. Slavin (2001), Global simulation of the Geospace Environment Modeling substorm challenge event, *J. Geophys. Res.*, *106*(A1), 381–395, doi:10.1029/2000JA000605.
Rankin, R., J. C. Samson, and V. T. Tikhonchuk (1999), Parallel electric fields in dispersive Alfvén waves in the dipolar magnetosphere, *Geophys. Res. Lett.*, *26*(24), 3601–3604, doi:10.1029/1999GL010715.
Roth, M., D. S. Evans, and J. Lemaire (1993), Theoretical structure of a magnetospheric plasma boundary: Application to the formation of discrete auroral arcs, *J. Geophys. Res.*, *98*(A7), 11,411–11,423, doi:10.1029/93JA00156.
Samson, J. C., L. R. Lyons, P. T. Newell, F. Creutzberg, and B. Xu (1992), Proton aurora and substorm intensifications, *Geophys. Res. Lett.*, *19*(21), 2167–2170, doi:10.1029/92GL02184.
Sato, T. (1978), A theory of quiet auroral arcs, *J. Geophys. Res.*, *83*(A3), 1042–1048, doi:10.1029/JA083iA03p01042.
Sazykin, S., R. A. Wolf, R. W. Spiro, T. I. Gombosi, D. L. De Zeeuw, and M. F. Thomsen (2002), Interchange instability in the inner magnetosphere associated with geosynchronous particle flux decreases, *Geophys. Res. Lett.*, *29*(10), 1448, doi:10.1029/2001GL014416.
Sergeev, V. A., V. Angelopoulos, J. T. Gosling, C. A. Cattell, and C. T. Russell (1996), Detection of localized, plasma-depleted flux tubes or bubbles in the midtail plasma sheet, *J. Geophys. Res.*, *101*(A5), 10,817–10,826, doi:10.1029/96JA00460.
Sergeev, V. A., K. Liou, C.-I. Meng, P. T. Newell, M. Brittnacher, G. Parks, and G. D. Reeves (1999), Development of auroral streamers in association with impulsive injections to the inner magnetotail, *Geophys. Res. Lett.*, *26*(3), 417–420, doi:10.1029/1998GL900311.
Sergeev, V. A., et al. (2000), Multiple-spacecraft observation of a narrow transient plasma jet in the Earth's plasma sheet, *Geophys. Res. Lett.*, *27*(6), 851–854, doi:10.1029/1999GL010729.
Sergeev, V., V. Angelopoulos, M. Kubyshkina, E. Donovan, X.-Z. Zhou, A. Runov, H. Singer, J. McFadden, and R. Nakamura (2011), Substorm growth and expansion onset as observed with ideal ground-spacecraft THEMIS coverage, *J. Geophys. Res.*, *116*, A00I26, doi:10.1029/2010JA015689.
Shi, Q., et al. (2013), Solar wind entry into the high-latitude terrestrial magnetosphere during geomagnetically quiet times, *Nat. Commun.*, *4*, 1466.
Shiokawa, K., K. Yumoto, K. Hayashi, T. Oguti, and D. J. McEwen (1995), A statistical study of the motions of auroral arcs in the high-latitude morning sector, *J. Geophys. Res.*, *100*(A11), 21,979–21,985, doi:10.1029/95JA01564.
Shiokawa, K., T. Ogino, K. Hayashi, and D. J. McEwen (1997), Quasi-periodic poleward motions of morningside Sun-aligned arcs: A multievent study, *J. Geophys. Res.*, *102*(A11), 24,325–24,332, doi:10.1029/97JA02383.
Shiokawa, K., G. Haerendel, and W. Baumjohann (1998), Azimuthal pressure gradient as driving force of substorm currents, *Geophys. Res. Lett.*, *25*(7), 959–962, doi:10.1029/98GL00540.
Stepanova, M. V., E. E. Antonova, J. M. Bosqued, R. A. Kovrazhkin, and K. R. Aubel (2002), Asymmetry of auroral electron precipitations and its relationship to the substorm expansion phase onset, *J. Geophys. Res.*, *107*(A7), 1134, doi:10.1029/2001JA003503.
Streltsov, A. V., and W. Lotko (1995), Dispersive field line resonances on auroral field lines, *J. Geophys. Res.*, *100*, 19,457–19,472, doi:10.1029/95JA01553.
Tanaka, T. (1994), Finite volume TVD scheme on an unstructured grid system for three-dimensional MHD simulation of inhomogeneous systems including strong background potential fields, *J. Comput. Phys.*, *111*, 381, doi:10.1006/jcph.1994.1071.
Tanaka, T. (2007), Magnetosphere-ionosphere convection as a compound system, *Space Sci. Rev.*, *133*, 1, doi:10.1007/s11214-007-9168-4.
Tanaka, T. (2015), Substorm auroral dynamics reproduced by the advanced global M-I coupling simulation, in *Auroral Dynamics and Space Weather*, *Geophys. Monogr. Ser.*, vol. 215, edited by Y. Zhang and L. J. Paxton, 177 pp., AGU, Washington, D. C.
Tanaka, T., T. Obara, and M. Kunitake (2004), Formation of the theta aurora by a transient convection during northward interplanetary magnetic field, *J. Geophys. Res.*, *109*, A09201, doi:10.1029/2003JA010271.
Tanaka, T., A. Nakamizo, A. Yoshikawa, S. Fujita, H. Shinagawa, H. Shimazu, T. Kikuchi, and K. K. Hashimoto (2010), Substorm convection and current system deduced from the global simulation, *J. Geophys. Res.*, *115*, A05220, doi:10.1029/2009JA014676.
Terada, N., H. Shinagawa, T. Tanaka, K. Murawski, and K. Terada (2009), A three-dimensional, multispecies, comprehensive MHD model of the solar wind interaction with the planet Venus, *J. Geophys. Res.*, *114*, A09208, doi:10.1029/2008JA013937.
Timofeev, E. E., and Y. I. Galperin (1991), Convection and currents in stable auroral arcs and inverted-V's, *J. Geomagn. Geoelectr.*, *43*(Suppl), 259–274.
Tóth, G., D. L. De Zeeuw, T. I. Gombosi, W. B. Manchester, A. J. Ridley, I. V. Sokolov, and I. I. Roussev (2007), Sun-to-thermosphere simulation of the 28–30 October 2003 storm with the Space Weather Modeling Framework, *Space Weather*, *5*, S06003, doi:10.1029/2006SW000272.
Valladares, C. E., H. C. Carlson Jr., and K. Fukui (1994), Interplanetary magnetic field dependency of stable Sun-aligned polar cap arcs, *J. Geophys. Res.*, *99*(A4), 6247–6272, doi:10.1029/93JA03255.
Watanabe, K., M. Ashour-Abdalla, and T. Sato (1986), A numerical model of the magnetosphere-ionosphere coupling: Preliminary results, *J. Geophys. Res.*, *91*(A6), 6973–6978, doi:10.1029/JA091iA06p06973.
White, W. W., G. L. Siscoe, G. M. Erickson, Z. Kaymaz, N. C. Maynard, K. D. Siebert, B. U. Ö. Sonnerup, and D. R. Weimer (1998), The magnetospheric sash and cross-tail S, *Geophys. Res. Lett.*, *25*(10), 1605–1608, doi:10.1029/98GL50865.
Wiltberger, M., T. I. Pulkkinen, J. G. Lyon, and C. C. Goodrich (2000), MHD simulation of the magnetotail during the December 10, 1996, substorm, *J. Geophys. Res.*, *105*(A), 27,649–27,664, doi:10.1029/1999JA000251.
Xing, X., L. R. Lyons, Y. Nishimura, V. Angelopoulos, E. Donovan, E. Spanswick, J. Liang, D. Larson, C. Carlson, and U. Auster (2011), Near-Earth plasma sheet azimuthal pressure gradient and associated auroral development soon before substorm onset, *J. Geophys. Res.*, *116*, A07204, doi:10.1029/2011JA016539.
Yahnin, A. G., V. A. Sergeev, B. B. Gvozdevsky, and S. Vennerstrom (1997), Magnetospheric source region of discrete auroras inferred from their relationship with isotropy boundaries of energetic particles, *Ann. Geophys.*, *15*, 943–958, doi:10.1007/s00585-997-0943-z.
Yao, Z. H., et al. (2012), Mechanism of substorm current wedge formation: THEMIS observations, *Geophys. Res. Lett.*, *39*, L13102, doi:10.1029/2012GL052055.
Yu, Y., A. J. Ridley, D. T. Welling, and G. Tóth (2010), Including gap region field-aligned currents and magnetospheric currents in the MHD calculation of ground-based magnetic field perturbations, *J. Geophys. Res.*, *115*, A08207, doi:10.1029/2009JA014869.
Zesta, E., L. R. Lyons, and E. Donovan (2000), The auroral signature of earthward flow burst observed in the magnetotail, *Geophys. Res. Lett.*, *27*(20), 3241–3244, doi:10.1029/2000GL000027.

京都大学 KYOTO UNIVERSITY
A Self-archived copy in
Kyoto University Research Information Repository
https://repository.kulib.kyoto-u.ac.jp
京都大学学術情報リポジトリ KURENAI 紅 Kyoto University Research Information Repository

Zesta, E., E. Donovan, L. Lyons, G. Enno, J. S. Murphree, and L. Cogger (2002), Two-dimensional structure of auroral poleward boundary intensifications, *J. Geophys. Res.*, *107*(A11), 1350, doi:10.1029/2001JA000260.

Zesta, E., L. Lyons, C.-P. Wang, E. Donovan, H. Frey, and T. Nagai (2006), Auroral poleward boundary intensifications (PBIs): Their two-dimensional structure and associated dynamics in the plasma sheet, *J. Geophys. Res.*, *111*, A05201, doi:10.1029/2004JA010640.